X International Conference on Textile Composites and Inflatable Structures
STRUCTURAL MEMBRANES 2021
K.-U.Bletzinger, E. Oñate, R. Wüchner and C. Lázaro (Eds)

FINITE ELEMENT MODELS TO SIMULATE LIGHTWEIGHT ROCKFALL PROTECTION STRUCTURES

Klaus B. Sautter[*†], Helene Hofmann[¶], Corinna Wendeler[§], Miguel Angel Celigueta[‡], Philipp Bucher[†], Kai-Uwe Bletzinger[†] and Roland Wüchner[†,‡]

[†]Technical University of Munich (TUM), Chair of Structural Analysis
Arcisstr. 21, D-80333 Mnchen, Germany
e-mail: klaus.sautter@tum.de, web page: www.st.bgu.tum.de

[‡]Centre Internacional de Mètodes Numèrics en Enginyeria (CIMNE)
Campus Nord UPC, 08034 Barcelona, Spain

[¶] Geobrugg AG, Aachstr. 11, Romanshorn 8590, Switzerland

[§] Appenzell Ausserrhoden, Department of Construction and Economics, Civil Engineering Office, Hydraulic Engineering, Kasernenstr. 17A, Herisau 9102, Switzerland

Key words: FEM, DEM, Particle Method, Impact, Rockfall, Natural Hazard, Protection Structures, Modeling

Abstract. Rockfall protection systems are highly flexible structures that can absorb large amounts of energy. Compared to rigid protection structures, these structures undergo large deformations upon impact and thus result in lower braking accelerations. This leads to an effective transfer of the load. Previous works have shown that the partly highly complicated real ring structures and rope constructions can be represented by simplified structural models, using the Finite Element Method (FEM), if the global behavior of the protective structure and the impacting objects is of interest. We discuss the appropriate modeling of the protective structures and sliding edge cables using the FEM in this work. Additionally the realization of the impact simulation by coupling particle methods and the FEM is briefly discussed.

1 INTRODUCTION

Rockfall protection systems can be found wherever vulnerable areas need to be protected. It is mainly roads along steep rock faces and settlements in mountainous landscapes that need to be protected accordingly. The protective structures are designed in such a way that they allow very large deformations in order to minimize the braking accelerations of the impacting objects. This allows for the efficient absorption and dissipation of large energies. In order to evaluate new designs, time-consuming and expensive

experiments have to be carried out. This testing process is to be supported by numerical computer simulation in order to make it cheaper and more effective. The basis and first investigations for the realization of such simulation is given in [8]. Since then, many other publications [8, 9, 10, 11, 12, 13] have dealt with and advanced this topic. In order to model the structure appropriately with the Finite Element Method (FEM), very detailed structural elements are developed, as can be read in [13], for example. The impacting objects are also discretized with finite elements (surfaces, lines) and finally the impact is simulated with suitable contact conditions. In order to avoid these complex contact algorithms (contact between surface and surface or surface and line, etc.) and to offer a modular simulation environment, recently published works [1, 2, 3, 4] have proposed to use the Discrete Element Method (DEM) to model the impacting objects while the structural response is still calculated by the FEM. The impacting objects are modeled from clusters of spherical single particles to approximate the irregular geometry of rocks while using the effective contact algorithm for spheres. Initial discussions of this coupling idea were published in [4] while the foundation for it was laid in [3] and is based on the work of [14, 15]. Practical applications and comparisons with experiments can be found in [1, 2]. The present paper will not deal with the implementation of the coupling and will instead focus on the modeling of the FEM model of the structure. Some of the more important element formulations and possible alternatives will be discussed. This paper can be seen as a short review article of selected passages from [1, 2, 3, 4].

2 Coupling Procedure

To realize the coupled simulation the multi-physics code KRATOS [16, 17, 18] is used. The DEM code and the FEM code are subsequently called and data is exchanged in a suitable co-simulation environment. The coupling procedure shall not be discussed in this work and the reader is kindly re-directed to [3]. Since structural modeling is to be discussed in this paper, we cannot avoid presenting the rough working of the coupling. The basic idea is to consider the structural domain both as a rigid boundary Ω_D in the DEM simulation and as a structural model Ω_S in the FEM simulation. The contact forces are calculated on Ω_D and then set to the appropriate nodes in the structural model Ω_S. A structural response is then calculated with the help of the FEM. The resulting solutions, such as displacements and velocities, are then set back to Ω_D and its coordinates are updated accordingly. By progressing in time in this way, the coupled simulation can be realized.

This modular approach has several advantages, with the different modeling of the interface in the DEM and the FEM being particularly noteworthy in the context of this work. As shown in Figure 1, for wire meshes, the rigid boundary Ω_D of the DEM can be modeled realistically with suitable openings while the structural model can use a simplified homogenized finite element model to describe Ω_S and thus offer an effective analysis tool. Figure 2 demonstrates the aforementioned coupling procedure and shows how small particles are able to penetrate the interface, although a homogenized FE model

is applied to calculate the structural response.

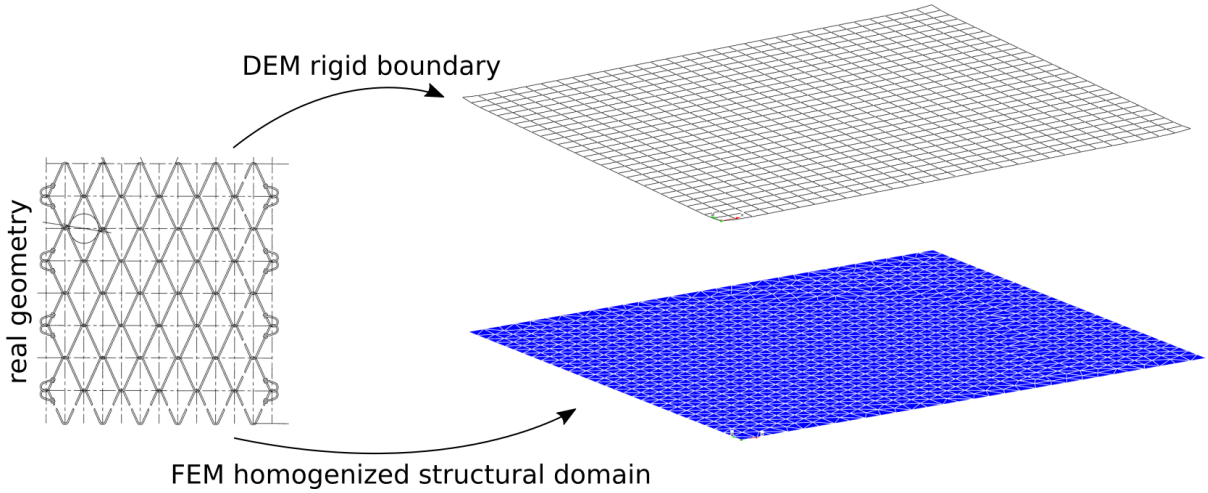

Figure 1: Discretization of the respective interface participants. The real geometry (adapted from [5]) is modeled realistically including any openings as the DEM rigid boundary. The model for calculating the structural response with the help of the FEM, on the other hand, is a simplified, homogenized surface that is discretized with triangular elements.

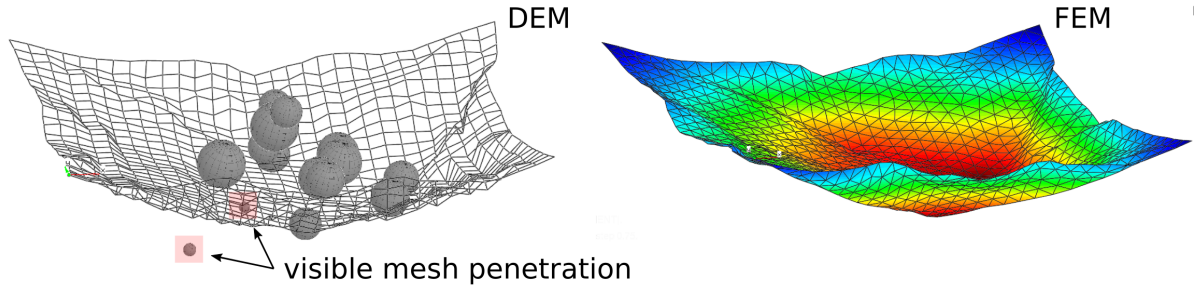

Figure 2: Visualization of the interface during impact. While the rigid boundary of the DEM allows for penetration of small impacting objects, the homogenized structural surface model allows for a simplified structural analysis of the deformation behavior applying the FEM.

Of course, one is not limited to modeling Ω_S by a homogenized FE model. If necessary, more detailed structural models can also be used.

3 DEM

More information on the DEM and its individual components can be found in [14, 15], for example.

4 FEM

The FEM is used to numerically solve partial differential equations. Since it is usually impossible to find closed-form solutions to most structural problems, the domain of the structure is divided into finite elements for which approximate solutions are available. This discretization allows to find a solution for the whole domain, which is evaluated at the discrete mesh nodes.

For an arbitrary structural domain, including Neumann and Dirichlet boundary conditions the strong form of the initial boundary value problem can be written as (not stating the boundary conditions),

$$div\,(\boldsymbol{\sigma}) + \mathbf{b} = \rho\ddot{\mathbf{u}}, \tag{1}$$

including the Cauchy stress tensor $\boldsymbol{\sigma}$, body forces $\mathbf{b}$, the density ρ and the accelerations $\ddot{\mathbf{u}}$. Multiplying Equation 1 with the virtual displacement field $\delta\mathbf{u}$ as the test function and integrating it over the current domain Ω, the weak form is achieved, expressing the virtual work. The virtual internal work δW_{int} is given in the following for both the current domain Ω and the initial domain Ω_0.

$$\delta W_{int} = \int_{\Omega} \boldsymbol{\sigma} : \delta\boldsymbol{\varepsilon}_{EA}\, d\Omega = \int_{\Omega_0} \mathbf{S} : \delta\boldsymbol{\varepsilon}_{GL}\, d\Omega_0. \tag{2}$$

The Euler-Almansi strain tensor $\boldsymbol{\varepsilon}_{EA}$, the Piola-Kirchhoff 2 (PK2) stress tensor $\mathbf{S}$ and its work conjugate Green-Lagrange strain tensor $\boldsymbol{\varepsilon}_{GL}$ are used. Bold letters indicate tensors of first and second order. Equation 2 is the starting point of most element formulations.

4.1 Sliding Edge Cable

One of the most important parts of the FE model is the sliding edge cable. It is one of the crucial components allowing for large deformations. The basic idea is to have an edge cable that allows all connecting nodes to slide along its axis, only restricted by friction. Three different methods have been investigated to realize the sliding along a deformable cable element, which are summarized in Table 1. Two of the methods, the penalty method [19] and multi point constraints [20] need a nearest neighbor search in each time step to search for the nearest two nodes along the edge cable to which the sliding constraint is either approximated or enforced. The third option, the sliding cable element formulation is a stand-alone element formulation that incorporates an arbitrary number of inner nodes along the edge cable which is only one single FE.

4.1.1 Sliding Cable Formulation

The finite element formulation for the sliding cable uses only one single element along the whole edge with the inner part discretized as shown in Figure 3. The idea is to calculate the internal stresses w.r.t. the change of the total length l instead of the change

	Advantages +	Drawbacks -
Sliding Edge Element Formulation	Efficient handling of friction Easy incorporation into FE model No neighbor search Edge cable is only 1 element Constraint exactly enforced	Implementation of new element
Penalty Method	No add. element implementation	Handling of friction Neighbor search Penalty factor Constraint only approximated
Multi Point Constraints	No add. element implementation Constraint exactly enforced	Handling of friction Neighbor search Case-by-case analysis necessary Non-linear constraint

Table 1: Advantages and drawbacks of three different methods to realize sliding along a given deformable cable element.

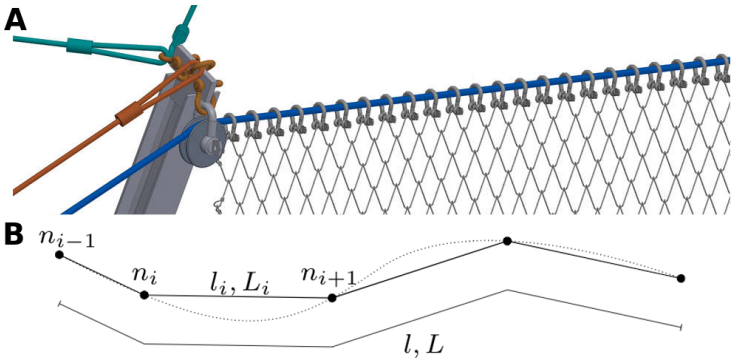

Figure 3: Support rope, taken from [1]. (A) Detailed sketch of installation guide, adapted from [6]. (B) Discretization of FEM model.

of the line segments l_i. A detailed derivation is given in [21] and shortly introduced in the following.

W.r.t. Equation 2, δW_{int} is expressed using the cross-section A, the total current length $l = \sum_i^{n_{lines}} l_i$, the total reference length $L = \sum_i^{n_{lines}} L_i$, the one-dimensional Green-Lagrange strain ε_{GL}, the one dimensional PK2 stress S, a given PK2 pre-stress S_{pre}, and a direction vector $\mathbf{T}$,

$$\delta W_{int} = \frac{l}{L} \cdot A \cdot (E \cdot \varepsilon_{GL} + S_{pre}) \cdot \mathbf{T} \cdot \delta \mathbf{u}, \tag{3}$$

$$\mathbf{T}_1 = \left[-\frac{\Delta x_1}{l_1} \quad -\frac{\Delta y_1}{l_1} \quad -\frac{\Delta z_1}{l_1} \right], \mathbf{T}_i = \left[\frac{\Delta x_{i-1}}{l_{i-1}} - \frac{\Delta x_i}{l_i} \quad \frac{\Delta y_{i-1}}{l_{i-1}} - \frac{\Delta y_i}{l_i} \quad \frac{\Delta z_{i-1}}{l_{i-1}} - \frac{\Delta z_i}{l_i} \right],$$
$$\mathbf{T}_{n_{nodes}} = \left[\frac{\Delta x_{n_{nodes}-1}}{l_{n_{nodes}-1}} \quad \frac{\Delta y_{n_{nodes}-1}}{l_{n_{nodes}-1}} \quad \frac{\Delta z_{n_{nodes}-1}}{l_{n_{nodes}-1}} \right]. \tag{4}$$

$\mathbf{T}$ contains the distance between the nodes, e.g. $\Delta x_i = x_{i+1} - x_i$. As described by [21, 8] an additional friction force can be easily added to the sum of internal forces at each node to model the movement restriction due to friction. Figure 4 demonstrates a test-setup for a coupled simulation applying the sliding element formulation.

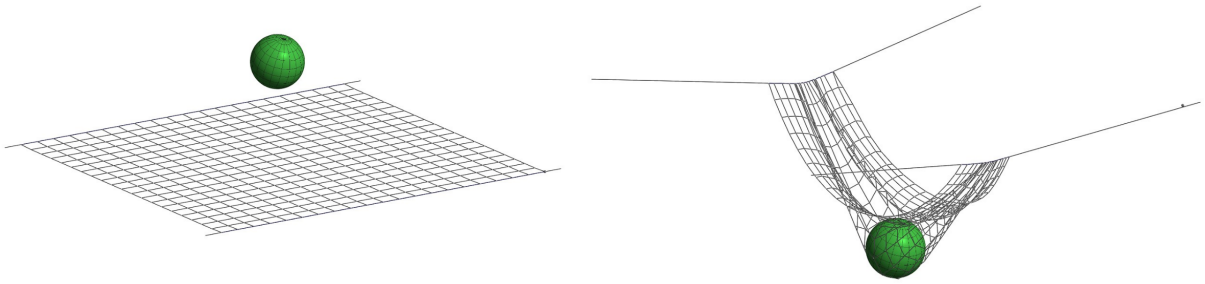

Figure 4: Impact simulation with sliding edge cables, taken from [3, 4]. The interior structural domain is modeled with standard cable elements.

4.1.2 Penalty Method

To realize the sliding with the help of the penalty method additional terms are added to the internal energy which represent an energy representation of the distance d between an arbitrary node and the edge cable segment. By minimizing the total internal energy in the FEM solving process the distance d is minimized too. W.r.t. Figure 5 the distance d can be calculated depending on the discrete nodal displacements $\mathbf{u}$ as follows:

$$\mathbf{v} = \mathbf{A}(\mathbf{u}) - \mathbf{C}(\mathbf{u}), \qquad \mathbf{w} = \mathbf{B}(\mathbf{u}) - \mathbf{A}(\mathbf{u})$$
$$d(\mathbf{u}) = \frac{|\mathbf{v} \times \mathbf{w}|}{|\mathbf{w}|}, \qquad d^2(\mathbf{u}) = \frac{(\mathbf{v} \times \mathbf{w}) \cdot (\mathbf{v} \times \mathbf{w})}{\mathbf{w} \cdot \mathbf{w}}. \tag{5}$$

d^2 is now used to define a functional f which is similar to the energy description of a single spring element,

$$f(\mathbf{u}) = \frac{1}{2} \cdot d^2(\mathbf{u}) \cdot \alpha, \tag{6}$$

where α represents the penalty factor which is highly problem dependent. By adding f to the total energy of the system the following contributions to the internal forces $F_{int,r}$ and

the tangential stiffness matrix $K_{r,s}$ can be expressed, while r, s are two arbitrary degrees of freedom.

$$F_{int,r} = \frac{\partial f}{\partial u_r} = \alpha \cdot \frac{\partial d}{\partial u_r}, \qquad K_{r,s} = \frac{\partial^2 f}{\partial u_r \partial u_s} = \alpha \cdot \frac{\partial^2 d}{\partial u_r \partial u_s}. \tag{7}$$

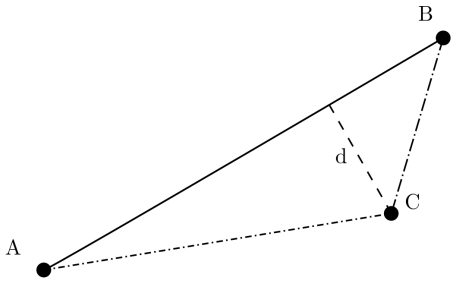

Figure 5: Visualization of the geometric investigations to determine the distance between an arbitrary node **C** and a line spanned between **A** and **B**.

The same simulation as shown in Figure 4 is repeated by replacing the sliding cable elements with standard cable elements and applying the penalty method. The final results are shown in Figure 6. It can be clearly seen, that there is a gap between the outer nodes and the edge cable. This is a result of the choice of the penalty factor α. If it is chosen wrongly it can either lead to badly conditioned system matrices (α is too large) or to a bad representation of the distance constraint (α is too low). This drawback makes the penalty method inferior to the sliding cable formulation for the problem setup at hand.

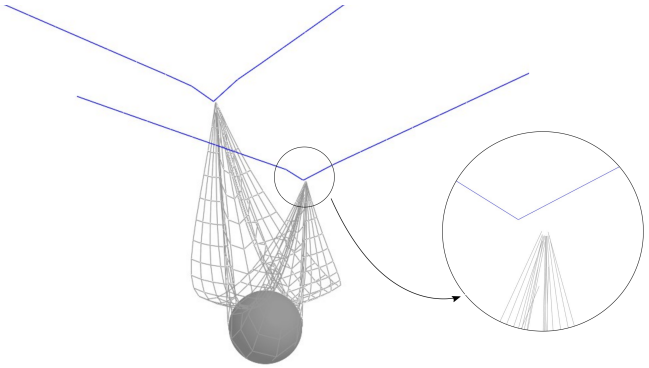

Figure 6: Impact simulation with standard cable elements on the interior and along the edges. The sliding is realized via the penalty method as described in this subsection 4.1.2.

4.1.3 Multi Point Constraint

In contrast to the penalty approach the Multi-Point constraint approach, aims to exactly reproduce the given constraint instead of approximating it. For this purpose a slave node and two master nodes are considered and their respective dofs are set in a specific relation. To obtain this relation the following Figure 7 is used.

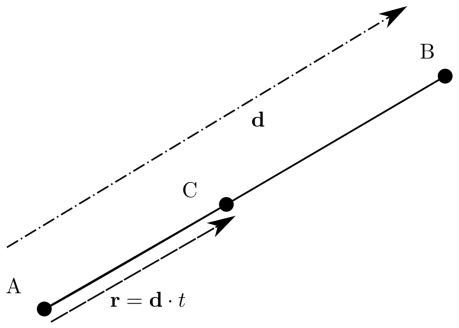

Figure 7: Visualization of the geometric investigations to determine the movement of an arbitrary node **C** on a line segment spanned between the nodes **A** and **B**.

The slave node **C** is only allowed to move along the line between master node **A** and **B**. The 3-dimensional line equation,

$$\begin{aligned} \mathbf{d} = \mathbf{B} - \mathbf{A} = \mathbf{B}_0 + \mathbf{u}_B - \mathbf{A}_0 - \mathbf{u}_A, \\ \mathbf{r} = \mathbf{C} - \mathbf{A} = \mathbf{C}_0 + \mathbf{u}_C - \mathbf{A}_0 - \mathbf{u}_A = t \cdot \mathbf{d}, \end{aligned} \tag{8}$$

can be used to express the respective displacement relations with an arbitrary scalar value t,

$$t = r_x/d_x = r_y/d_y = r_z/d_z. \tag{9}$$

The further procedure is described below as an example for case $d_x \neq 0$ and only the y-displacement v_C, whereby case distinctions are necessary depending on the problem. First the relations between the displacements are expressed,

$$if \quad d_x \neq 0 \rightarrow \quad r_y = r_x \cdot \frac{d_y}{d_x} \quad \wedge \quad r_z = r_x \cdot \frac{d_z}{d_x}, \tag{10}$$

which allows the expression of the respective master-slave relations with the x-displacement u, y-displacement v, and z-displacement w,

$$\underbrace{v_C}_{\text{slave}} = Y_A + \underbrace{v_A}_{\text{master}} - Y_C + \left[\left(X_C + \underbrace{u_C}_{\text{master}} - X_A - \underbrace{u_A}_{\text{master}} \right) \cdot \frac{Y_B + \overbrace{v_B}^{\text{master}} - Y_A - \overbrace{v_A}^{\text{master}}}{X_B + \underbrace{u_B}_{\text{master}} - X_A - \underbrace{u_A}_{\text{master}}} \right]. \tag{11}$$

Obviously, Equation 11 is a non-linear constraint and in the following exemplary linearized, while d_X, d_Y in Equation 12 are considered to be constant and given by the last time step,

$$d_X = X_B + u_B - X_A - u_a, \quad d_Y = Y_B + v_B - Y_A - v_a, \tag{12}$$

$$\underbrace{v_C}_{\text{slave}_1} = \underbrace{\left(Y_A - Y_C + \frac{Y_B - Y_A}{d_X} \cdot (X_C - X_A)\right)}_{\text{constant}} + \underbrace{v_A}_{\text{master}_1} \cdot \underbrace{\left(1 + \frac{X_A - X_C}{d_X}\right)}_{\text{weight}_1} + \underbrace{v_B}_{\text{master}_2} \cdot \underbrace{\frac{X_C - X_A}{d_X}}_{\text{weight}_2} + \underbrace{u_C}_{\text{master}_3} \cdot \underbrace{\frac{d_Y}{d_X}}_{\text{weight}_3} - \underbrace{u_A}_{\text{master}_4} \cdot \underbrace{\frac{d_Y}{d_X}}_{\text{weight}_4}. \tag{13}$$

Finally, after successfully declaring all proper constraints the system stiffness matrix $\mathbf{K}$ must be transformed by $\hat{\mathbf{K}} = \mathbf{\Lambda}^T \mathbf{K} \mathbf{\Lambda}$, with the help of $\mathbf{\Lambda}$ containing the constraint information. In the case of an explicit dynamic simulation in which the accelerations $\ddot{\mathbf{u}} = \mathbf{M}^{-1} \cdot (\mathbf{res} - \mathbf{D} \cdot \dot{\mathbf{u}})$, with the mass matrix $\mathbf{M}$, the force residual $\mathbf{res}$, the velocities $\dot{\mathbf{u}}$, and the damping matrix $\mathbf{D}$ are solved, the residual must be manipulated to $\mathbf{res}_{master} = \mathbf{res}_{master} + \mathbf{res}_{slave} \cdot weight$.

The complexity of this method and the additional drawbacks shown in Table 1 make this method again inferior to the sliding edge cable formulation for this problem.

4.2 Plate In Membrane Action with Tension Field Theory

As demonstrated in Figure 1 the complex wire mesh geometries of some protection nets can be simplified in the numerical FE model with an homogenized surface model. In this work plane stress plates in membrane action are used, which has been proven to be applicable for the aforementioned structures [3, 1]. In order to do justice to the anisotropic material behavior of wire meshes, the Münsch and Reinhardt [22] law can be used, for example. It allows the definition of two different Young's-Moduli E_x, E_y and is therefore suitable for the problems at hand. The anisotropic elastic consistent linearized tangent modulus $\mathbb{C}$ is expressed with the two Poisson's ratios ν_{yx}, ν_{xy} and the shear modulus G,

$$\mathbb{C} = \frac{1}{1 - \nu_{xy}\nu_{yx}} \begin{bmatrix} E_x & \nu_{xy}E_x & 0 \\ \nu_{yx}E_y & E_y & 0 \\ 0 & 0 & (1 - \nu_{xy}\nu_{yx})\, G \end{bmatrix}, \quad \frac{\nu_{xy}}{E_y} = \frac{\nu_{yx}}{E_x}. \tag{14}$$

Figure 8 shows the same simulation as done in Figure 4 by replacing the inner cable net model with plate in membrane action elements. It can be seen, that although sliding edge cables are applied the compression stresses in the plate elements prevent the structure from a realistic deformation behavior.

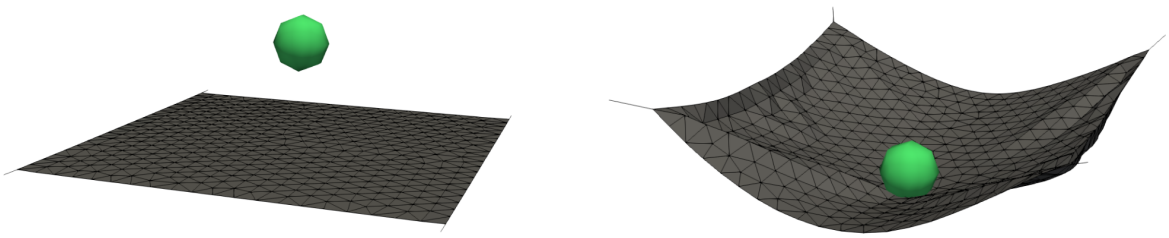

Figure 8: Impact simulation with sliding edge cables. The interior structural domain is modeled with plate in membrane action elements, which can carry compression forces.

As a remedy the tension field theory is applied, which is described in [7]. It checks for the principal stresses by an eigen-value analysis and transforms $\mathbb{C}$ if compression stresses are detected. This way the correct deformation behavior is replicated, by excluding compression stresses, which is shown in Figure 9.

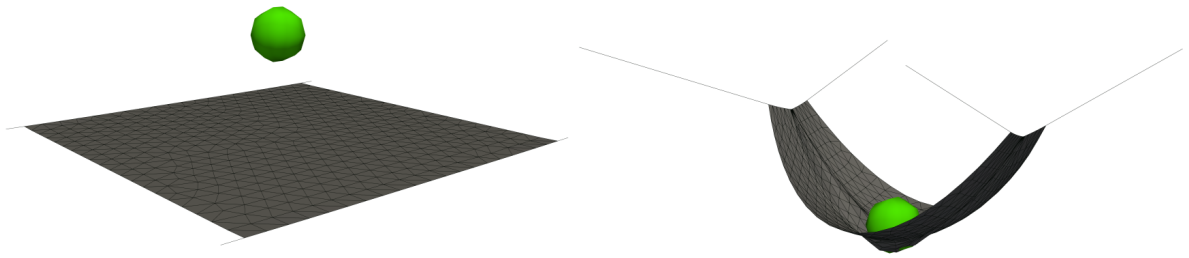

Figure 9: Impact simulation with sliding edge cables, adapted from [1]. The interior structural domain is modeled with plate in membrane action elements applying the tension field theory, described by [7], which excludes compression stresses.

5 CONCLUSIONS

In order to simulate the highly non-linear interaction between impacting objects and protective structures for rockfalls, we couple the DEM and the FEM. A brief introduction to the coupling procedure has been given in this paper, with reference to [3] for further information. Both the correct modeling of the rock [2] and the appropriate structural modeling must be done carefully. This paper discusses some important aspects of structural modeling using the FEM. Two structural elements that need special attention in the model of the protective structure have been discussed and possible alternatives were pointed out. The application of the models presented here can be found in [1, 2].

REFERENCES

[1] K. B. Sautter, H. Hofmann, C. Wendeler, P. Wilson, P. Bucher, K.-U. Bletzinger, and R. Wüchner *Advanced modeling and simulation of rockfall Attenuator barriers via partitioned DEM-FEM coupling*, Frontiers in Built Environment - Computational Methods in Structural Engineering, (2021)

[2] K. B. Sautter, H. Hofmann, C. Wendeler, R. Wüchner, and K.-U. Bletzinger, *Influence of the refinement of DE-Clusters with regard to the numerical analysis of rock-fall experiments*, Computational Particle Mechanics, (2021).

[3] K. B. Sautter, T. Teschemacher, M. A. Celigueta, P. Bucher, K.-U. Bletzinger, and R. Wüchner, *Partitioned strong coupling of discrete elements with large deformation structural finite elements to model impact on highly flexible tension structures*, Advances in Civil Engineering, (2020)

[4] C. Wendeler, K. B. Sautter, P. Bucher, K.-U. Bletzinger, and R. Wüchner, *Modellierungsaspekte und gekoppelte DEM-FEM Simulationen zur Untersuchung hochflexibler Steinschlagschutznetze*, Berichte der Fachtagung Baustatik - Baupraxis 14, (2020)

[5] Geobrugg AG, 8590 Romanshorn, SPIDER®, www.geobrugg.com, (2020)

[6] Geobrugg AG, 8590 Romanshorn, System manual, Att-80, Attenuator System, (2019)

[7] Nakashino Kyoichi, Natori M. C., *Efficient Modification Scheme of Stress-Strain Tensor for Wrinkled Membranes*, AIAA Journal (2005)

[8] A. Volkwein, *Numerische Simulation von flexiblen Steinschlagschutzsystemen*, Ph.D. thesis, ETH (2004)

[9] A. Mentani, L. Govoni, A. Giacomini, G. Gottardi, and O. Buzzi, *An Equivalent Continuum Approach to Efficiently Model the Response of Steel Wire Meshes to Rockfall Impacts*, Rock Mechanics and Rock Engineering (2018)

[10] S. Tahmasbi, A. Giacomini, C. Wendeler, and O. Buzzi, *On the Computational Efficiency of the Hybrid Approach in Numerical Simulation of Rockall Flexible Chain-Link Mesh*, Rock Mechanics and Rock Engineering (2019)

[11] N. Sasiharan, B. Muhunthan, T.C. Badger, S. Shu, and D. M. Carradine, *Numerical analysis of the performance of wire mesh and cable net rockfall protection systems*, Engineering Geology (2006)

[12] S. Dhakhal, NP. Bhandary, R. Yatabe, and R. Kinoshita, *Experimental, numerical and analytical modelling of a newly developed rockfall protective cable-net structure*, Natural Hazards and Earth System Sciences (2011)

[13] J. P. Escallon, V. Boetticher, C. Wendeler, E. Chatzi, and P. Bartelt, *Mechanics of chain-link wire nets with loose connections*, Engineering Structures (2015)

[14] M. Santasusana, *Numerical Techniques for non-linear analysis of structures combining Discrete Element and Finite Element Methods*, Ph.D. thesis, CIMNE (2016)

[15] M. Santasusana, J. Irazábal, E. Oñate, and J.M. Carbonell, *The Double Hierarchy Method. A parallel 3D contact method for the interaction of spherical particles with rigid FE boundaries using the DEM*, Computational Particle Mechanics (2016)

[16] P. Dadvand, R. Rossi, and E. Oñate, *An Object-oriented Environment for Developing Finite Element Codes for Multi-disciplinary Applications*, Archives of Computational Methods in Engineering (2010)

[17] P. Dadvand, R. Rossi, M. Gil, X. Martorell, J. Cotela, E. Juanpere, S. Idelsohn and E. Oñate, *Migration of a generic multi-physics framework to HPC environments*, Computers & Fluids (2013)

[18] V. Mataix Ferrándiz, P. Bucher, R. Rossi, J. Cotela, J.M. Carbonell, R. Zorrilla and R. Tosi, *KratosMultiphysics (Version 8.0)*, Zenodo (2020)

[19] A. M. Bauer, R. Wüchner, and K.-U. Bletzinger, *Innovative CAD-integrated Isogeometric Simulation of Sliding Edge Cables in Lightweight Structures*, Journal of the International Association for Shell and Spatial Structures (2018)

[20] John F. Abel, and Mark S. Shephard, *An algorithm for multipoint constraints in finite element analysis*, International Journal for Numerical Methods in Engineering (1979)

[21] Romain Boulaud and Cyril Douthe, *A Sliding Cable Model for Rockfall Barrier Simulations Using Dynamic Relaxation*, IASS Annual Symposium (2017)

[22] Münsch, R. and Reinhardt, H.-W., *Zur Berechnung von Membrantragwerken aus beschichteten Geweben mit Hilfe genäherter elastischer Materialparameter*, Bauingenieur (1995)